Instantaneous Multi-Baseline Ambiguity Resolution with Constraints

P.J. Buist, P.J.G. Teunissen, G. Giorgi, S. Verhagen *Delft University of Technology*

P.J.Buist@tudelft.nl

ABSTRACT
Traditionally the relative positioning and attitude determination problem are treated as independent. In this contribution we will investigate the possibilities to use multi-antenna data, not only for attitude determination, but also for the relative positioning. The developed methods are rigorous and have an additional advantage that they improve the ambiguity resolution on the unconstrained baseline and the overall success rate of ambiguity resolution between a number of antennas.

1 INTRODUCTION
In this paper we will explore methods for the combination of both relative positioning and attitude determination for moving platforms, each platform having multi-antennas with known baseline lengths on its own surface, and baseline vectors with unknown length to the other platforms. The objective of this research is to develop a method that optimally makes use of all the information available (the integerness of the ambiguities, the relationship between the ambiguities on the different baselines and the known baseline length of the constrained baselines) to determine the relative position and orientation of a multi-antenna system with unconstrained and constrained baselines. We will develop a rigorous integrated method and investigate its ambiguity resolution performance on mainly the unconstrained baselines and the overall success rate of the ambiguity resolution between a number of antennas. The paper begins with some background information on potential applications. In section 3 a general model for unconstrained and constrained baselines is introduced. Section 4 describes the standard methods for ambiguity resolution for unconstrained (e.g. relative navigation) and constrained (e.g. attitude determination) baseline applications. Section 5 introduces three methods for multi-antenna ambiguity resolution and describes the methods mathematically. In section 6 the methods are tested using simulated and field data. The paper concludes with recommendations for future work and conclusions.

2 BACKGROUND
2.1 RELATIVE NAVIGATION
Currently precise relative navigation using GNSS is under development for a large number of applications on land, on the water, in the air and even in space. The automotive industry shows interest in this application for relative navigation between vehicles and reference stations, but also between vehicles. For maritime applications especially inshore relative navigation requires precise and robust methods. For formation flying of air- and spacecraft, obviously this kind of technique is required for a swarm of Unmanned Aerial Vehicles (UAV), but also for swarms of manned vehicles it could be beneficial. Other aircraft applications are aerial refueling as well as potentially landing. For relative navigation between aircraft and vessels, the landing on aircraft carriers is an important application. If the vehicles have multiple antennas, potentially GNSS could be used for determination of the attitude of the vehicle(s). Traditionally the relative positioning and attitude determination problem are treated as independent. In this contribution we will investigate the possibilities to use multi-antenna data, not only for attitude determination, but also to improve the relative positioning.

2.2 ABSOLUTE AND RELATIVE ATTITUDE DETERMINATION
Attitude determination using GNSS signals is becoming more and more accepted for real world applications. With 2 antennas/ 1 baseline, a direction similar to a magnetic compass can be estimated. With 3 antennas/2 baselines, placed at appropriate relative positions, the full attitude can be determined. For some applications we would like to know the relative attitude between two platforms, which also could

be provided by GNSS if both platforms have a number of antennas. Examples of these applications are aerial refueling, landing on aircraft carriers and rendezvous and docking in space, but also formation flying if the elements of the formation have to point in certain directions relative to each other.

3 MODELLING

3.1 MODEL FOR UNCONSTRAINED BASELINES

Precise GNSS receivers make use of two types of observations: pseudo range and carrier phase. The pseudo range observations typically have an accuracy of decimeters, whereas carrier phase observations have accuracies up to millimeter level. The double difference observation equations can be written as a system of linearized observation equations [1]:

$$E(y) = Aa + Bb, \quad D(y) = Q_y \qquad (1)$$

Where E is the mean or the expected value and D is the variance or dispersion of y. y is the vector of observed minus estimated double difference carrier phases and/or code observations of the order m, a is the unknown vector of ambiguities of the order n expressed in cycles rather than range to maintain their integer character, b is the baseline vector, which is unknown for relative navigation applications but for which the length in attitude determination is known, B is the geometry matrix containing normalized line-of-sight vectors, A is a design matrix that links the data vector to the unknown vector a. In this paper the assumption is made that the antennas are close to each other and thus atmospheric affects can be neglected. The variance matrix of y is given by the positive definite matrix Q_y which is assumed to be known. As explained in [1], the least squares solution of the linear system of observation equations as introduced in eq. (1) is obtained from:
$\min_{a,b} \|y - Aa - Bb\|_{Q_y}^2$, where $\|..\|_{Q_y}^2 = (..)^T Q_y^{-1}(..)$.

3.2 MODEL FOR CONSTRAINED BASELINES

For a baseline constrained application, as for example GNSS -based attitude determination, we can make use of the knowledge that the length of the baseline is known and constant. Hence the baseline constrained integer ambiguity resolution can make use of the standard GNSS model by adding the length constraint of the baseline $||b||_{I_3} = l$, where l is known. The observation equations then become [2]:

$$E(y) = Aa + Bb, \quad D(y) = Q_y,$$
$$||b||_{I_3} = l, \quad a \in \mathbb{Z}^n, \quad b \in \mathbb{R}^3 \qquad (2)$$

Using this transformation the least squares criterion reads

$$\min_{a \in \mathbb{Z}^n, b \in \mathbb{R}^3, ||b||_{I_3} = l} \|y - Aa - Bb\|_{Q_y}^2 \qquad (3)$$

This least squares problem is coined a Quadratically Constrained Integer Least Squares (QC-ILS) problem in [3].

4 AMBIGUITY RESOLUTION

High-precision positioning and attitude determination requires the use of the very precise GNSS carrier phase observations, which however are ambiguous by an unknown integer number of cycles. For ambiguity resolution we make use of the LAMBDA (Least-squares AMBiguity Decorrelation Adjustment) method and its recently developed baseline constrained extension [2]. This method will briefly be discussed.

4.1 THE STANDARD LAMBDA METHOD

The least squares criterion for the unconstrained problem reads as[1]:

$$\min_{a \in \mathbb{Z}^n, b \in \mathbb{R}^3} \|y - Aa - Bb\|_{Q_y}^2 = \|\hat{e}\|_{Q_y}^2 +$$
$$\min_{a \in \mathbb{Z}^n, b \in \mathbb{R}^3} \left(\|\hat{a} - a\|_{Q_{\hat{a}}}^2 + \|\hat{b}(a) - b\|_{Q_{\hat{b}(a)}}^2 \right) \qquad (4)$$

for which the last term can be made zero for any a, and where $\hat{e} = y - A\hat{a} - B\hat{b}$ is the least squares residual of the float solution $\hat{a}, \hat{b}$.
We solve the vector of integer least-squares estimates of the ambiguities $\check{a}$:

$$\check{a} = \arg(\min_{a \in \mathbb{Z}^n} \|\hat{a} - a\|_{Q_{\hat{a}}}^2) \qquad (5)$$

with $\arg$ is the vector of integers that minimize the term within the brackets. A so called integer search is needed to find $\check{a}$. The search space for this problem is defined as:

$$\Psi(\chi^2) = \left\{ a \in \mathbb{Z}^n | \|\hat{a} - a\|_{Q_{\hat{a}}}^2 \leq \chi^2 \right\} \qquad (6)$$

with χ^2 is a properly chosen constant. The LAMBDA method is an efficient way to do this [4][5][6].
Once the solution $\check{a}$ has been obtained, the residual $(\hat{a} - \check{a})$ is used to adjust the float solution $\hat{b}$ of the first step, and therefore the final fixed baseline solution is obtained as: $\check{b} = \hat{b}(\check{a}) = \hat{b} - Q_{\hat{b}\hat{a}} Q_{\hat{a}}^{-1} (\hat{a} - \check{a})$.

4.2 BASELINE CONSTRAINED LAMBDA METHOD

The least squares criterion for eq. (3) of the baseline constrained problem reads as:

$$\min_{\substack{a \in \mathbb{Z}^n, \\ b \in \mathbb{R}^3, \\ ||b|| = l}} \|y - Aa - Bb\|_{Q_y}^2 =$$

$$\|\hat{e}\|_{Q_y}^2 + \min_{a \in \mathbb{Z}^n} \left(\|\hat{a} - a\|_{Q_{\hat{a}}}^2 + \min_{\substack{b \in \mathbb{R}^3, \\ ||b|| = l}} \left(\|\hat{b}(a) - b\|_{Q_{\hat{b}(a)}}^2 \right) \right) \qquad (7)$$
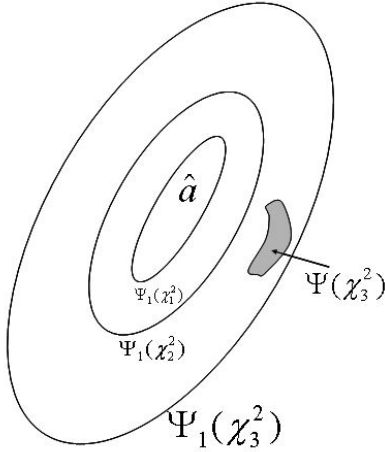
Fig. 1: Baseline constrained LAMBDA using "the Expanding approach"

where $\hat{b}(a)$ is the least squares solution for b, assuming that a is known and $Q_{\hat{b}(a)} = Q_{\hat{b}} - Q_{\hat{b}\hat{a}} Q_{\hat{a}}^{-1} Q_{\hat{a}\hat{b}}$.

In the constrained approach we will search for the integer least-squares ambiguity vector in the search space:

$$\Psi(\chi^2) = \left\{ a \in \mathbb{Z}^n \mid ||\hat{a} - a||^2_{Q_{\hat{a}}} + ||\hat{b}(a) - \check{b}(a)||^2_{Q_{\hat{b}(a)}} \leq \chi^2 \right\} \quad (8)$$

Where $\check{b}(a)$ is the fixed solution for b, assuming that a is known: $\check{b}(a) = \arg(\min_{b \in \mathbb{R}^n, ||b|| = l} ||\hat{b}(a) - b||^2_{Q_{\hat{b}(a)}})$. The method applied in this contribution, and in [7] and [8], is referred to as "the expanding approach". Another method developed to solve the same problem, the so called "Search and Shrink Method", is described in [9]. In the expanding approach, we first use the standard LAMBDA method to collect integer vectors inside the search space $\Psi_1(\chi^2) = \left\{ a \in \mathbb{Z}^n \mid ||\hat{a} - a||^2_{Q_{\hat{a}}} \leq \chi^2 \right\}$ and store all those that fullfill the inequality:

$$||\hat{b}(a) - \check{b}(a)||^2_{Q_{\hat{b}(a)}} \leq \chi^2 - ||\hat{a} - a||^2_{Q_{\hat{a}}} \quad (9)$$

The initial search space is defined as the value $\chi_1^2 = ||\hat{a} - \check{a}_B||^2_{Q_{\hat{a}}}$ with $\check{a}_B$ is the bootstrapped solution of $\hat{a}$ [10][11][5] [1]. This initial value is increased until the search space Ψ is non-empty, using the logic visualized in fig. 1. For every step we enumerate all the integer vectors contained in Ψ. If the set is non-empty, we pick up the minimizer, otherwise we increase the size of the search space. This process is very time efficient and typically takes less than 10 ms in a MATLAB environment at an Intel Core 2 CPU 6400 @ 2.13 GHz for the field data described in section 6.4.

5 BASELINE CONSTRAINED MULTI-ANTENNA AMBIGUITY RESOLUTION

Precise relative positioning of two moving platforms usually requires dual-frequency phase data, whereas - due to the baseline length constraints - single-frequency phase data may suffice for the precise determination of platform attitudes [7][8][12]. These two GNSS problems, relative positioning and attitude determination, are usually treated separately and independent from one another. In this contribution, however, we will combine the two problems and discuss different processing strategies for solving them. As such the problem becomes a multi-antenna ambiguity resolution problem of which some of the baseline lengths are constrained. The different strategies discussed range from the uncoupled approach to the fully integrated approach of [13]. Insight in the numerical and statistical properties of these different approaches will be given. First we will introduce a 3 baseline setup, which we will use to investigate the processing strategies theoretically. This 3 baseline setup is a simplified model that represents experiments as described in [8] and [12].

5.1 MULTI-BASELINE SETUP

As is shown in fig. 2, the unconstrained baselines between antenna 3 (Ant_3) (e.g. at one platform) and the antennas 1 (Ant_1) and 2 (Ant_2) (e.g. onboard another platform) are called baseline 2 (b_2) and baseline 3 (b_3) respectively. The constrained baseline is called baseline 1 (b_1). The three antennas are assumed to be sufficiently close so that the relative antenna-satellite geometry may be considered the same for all antennas. The design matrices A and B and the variance-covariance matrix Q_y are assumed to be identical. We take the ordering of the three antenna pairs such that y_1 is the difference of the single-differenced data of antenna 2 minus that of antenna 1, y_2 is the difference of the single difference data of antenna 3 minus that of antenna 2 and y_3 is the difference of the single difference of antenna 3 minus that of antenna 1.
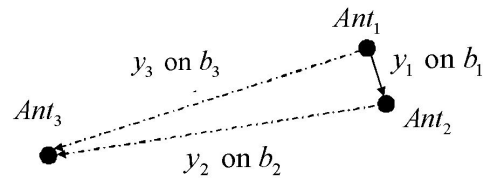
Fig. 2: Baseline definition

5.2 MODEL AND UNCONSTRAINED FLOAT SOLUTION

For an integrated approach, we can use the known relationship between constrained and unconstrained baselines. For constrained baseline b_1 and unconstrained baselines b_2, b_3

respectively, with common antennas we have the following relationship for the baseline, ambiguities and observation vectors:

$$b_3 = b_1 + b_2$$
$$a_3 = a_1 + a_2 \tag{10}$$
$$y_3 = y_1 + y_2$$

This equation shows that two out of three double difference data vectors are sufficient to set up the GNSS model. For the general solution of multi-baselines we can use eq. (4) for every baseline i.

If we use y_1 and y_2 the model becomes:

$$E \begin{bmatrix} y_1 \\ y_2 \end{bmatrix} = \begin{bmatrix} A & B & 0 & 0 \\ 0 & 0 & A & B \end{bmatrix} \begin{bmatrix} a_1 \\ b_1 \\ a_2 \\ b_2 \end{bmatrix},$$
$$D \begin{bmatrix} y_1 \\ y_2 \end{bmatrix} = \begin{bmatrix} Q_y & -\frac{1}{2}Q_y \\ -\frac{1}{2}Q_y & Q_y \end{bmatrix} \tag{11}$$

Note the presence of the nonzero covariance matrix $C(y_1, y_2) = -\frac{1}{2}Q_y$, which is due to the fact that the double difference vectors y_1 and y_2 have an antenna in common. Using the Kronecker symbol we can write the model in a more compact form:

$$E \begin{bmatrix} y_1 \\ y_2 \end{bmatrix} = I_2 \otimes (A, B) \begin{bmatrix} a_1 \\ b_1 \\ a_2 \\ b_2 \end{bmatrix}, D \begin{bmatrix} y_1 \\ y_2 \end{bmatrix} = P \otimes Q_y \tag{12}$$

with $P = \begin{bmatrix} 1 & -\frac{1}{2} \\ -\frac{1}{2} & 1 \end{bmatrix}$.

Application of the least squares principle to the above model gives the least squares solution and corresponding variance matrix as:

$$\begin{bmatrix} \hat{a}_1 \\ \hat{b}_1 \\ \hat{a}_2 \\ \hat{b}_2 \end{bmatrix} = \left[I_2 \otimes \left[(A, B)^T Q_y^{-1} (A, B) \right]^{-1} (A, B)^T Q_y^{-1} \right] \begin{bmatrix} y_1 \\ y_2 \end{bmatrix}$$

$$D \begin{bmatrix} \hat{a}_1 \\ \hat{b}_1 \\ \hat{a}_2 \\ \hat{b}_2 \end{bmatrix} = P \otimes \left[(A, B)^T Q_y^{-1} (A, B) \right]^{-1} \tag{13}$$

This shows that $\hat{a}_i$ and $\hat{b}_i$ are solely determined by the double difference vector of the corresponding antenna pair, i.e. y_i, thus parallel processing is possible for the float solution. In section 5.3, it will be demonstrated that this property is lost once the integer constraints are applied. If we denote the variance-covariance matrix of $\hat{a}_i$ and $\hat{b}_i$ as:

$$\left[(A, B)^T Q_y^{-1} (A, B) \right]^{-1} = \begin{bmatrix} Q_{\hat{a}} & Q_{\hat{b}\hat{a}} \\ Q_{\hat{b}\hat{a}} & Q_{\hat{b}} \end{bmatrix} \tag{14}$$

then

$$D \begin{bmatrix} \hat{a}_1 \\ \hat{b}_1 \\ \hat{a}_2 \\ \hat{b}_2 \end{bmatrix} = \left[P \otimes \begin{bmatrix} Q_{\hat{a}} & Q_{\hat{b}\hat{a}} \\ Q_{\hat{b}\hat{a}} & Q_{\hat{b}} \end{bmatrix} \right] \tag{15}$$

or

$$D \begin{bmatrix} \hat{a}_1 \\ \hat{a}_2 \\ \hat{b}_1 \\ \hat{b}_2 \end{bmatrix} = \begin{bmatrix} P \otimes Q_{\hat{a}} & P \otimes Q_{\hat{b}\hat{a}} \\ P \otimes Q_{\hat{b}\hat{a}} & P \otimes Q_{\hat{b}} \end{bmatrix} \tag{16}$$

If one wants to determine a_3 and b_3 from the above results it can be obtained from:

$$\begin{bmatrix} \hat{a}_3 \\ \hat{b}_3 \end{bmatrix} = \left[(1, 1) \otimes \begin{bmatrix} I_n & 0 \\ 0 & I_3 \end{bmatrix} \right] \begin{bmatrix} \hat{a}_1 \\ \hat{b}_1 \\ \hat{a}_2 \\ \hat{b}_2 \end{bmatrix} \tag{17}$$

Application of the variance propagation law shows that this solution has the same precision as the other baselines.

5.3 OPTIMAL SOLUTION OF THE FULLY INTEGRATED APPROACH (INTEGRATED APPROACH I)

For the derivation of the integer least squares solution, which is the optimal solution, we use the 3 baseline system introduced in section 5.1, for which the baseline b_1 is constrained and the baseline b_2 is unconstrained. First we write the sum-of-squares decomposition as:

$$\left\| \begin{matrix} y_1 - Aa_1 - Bb_1 \\ y_2 - Aa_2 - Bb_2 \end{matrix} \right\|^2_{P \otimes Q_y} =$$

$$\left\| \begin{matrix} \hat{e}_1 \\ \hat{e}_2 \end{matrix} \right\|^2_{P \otimes Q_y} + \left\| \begin{matrix} \hat{a}_1 - a_1 \\ \hat{a}_2 - a_2 \end{matrix} \right\|^2_{P \otimes Q_{\hat{a}}} + \left\| \begin{matrix} \hat{b}_1(a_1, a_2) - b_1 \\ \hat{b}_2(a_1, a_2) - b_2 \end{matrix} \right\|^2_{P \otimes Q_{\hat{b}(a)}} \tag{18}$$

The ambiguity-constrained baseline solution with variance-covariance matrix are given as:

$$\begin{bmatrix} \hat{b}_1(a_1, a_2) \\ \hat{b}_2(a_1, a_2) \end{bmatrix} =$$

$$\begin{bmatrix} \hat{b}_1 \\ \hat{b}_2 \end{bmatrix} - (P \otimes Q_{\hat{b}\hat{a}})(P \otimes Q_{\hat{a}})^{-1} \begin{bmatrix} \hat{a}_1 - a_1 \\ \hat{a}_2 - a_2 \end{bmatrix} = \begin{bmatrix} \hat{b}_1(a_1) \\ \hat{b}_2(a_2) \end{bmatrix} \tag{19}$$

and

$$D \begin{bmatrix} \hat{b}_1(a_1, a_2) \\ \hat{b}_2(a_1, a_2) \end{bmatrix} = P \otimes Q_{\hat{b}(a)} \tag{20}$$

Therefore we can conclude that knowledge about a_1 does not improve $\hat{b}_2(a_2)$ and similarly, knowledge about a_2 does not help to improve $\hat{b}_1(a_1)$.

In order to obtain the unknown parameters we need to solve the following minimization problem:

$$F(a_1, a_2, b_1, b_2) = \min_{\substack{a_1,a_2\in\mathbb{Z}^n, \\ b_1,b_2\in\mathbb{R}^3, \\ ||b_1||_{I_3}=l}} \left\| \begin{matrix} y_1 - Aa_1 - Bb_1 \\ y_2 - Aa_2 - Bb_2 \end{matrix} \right\|^2_{P\otimes Q_y} =$$

$$\left\| \begin{matrix} \hat{e}_1 \\ \hat{e}_2 \end{matrix} \right\|^2_{P\otimes Q_y} +$$

$$+ \min_{\substack{a_1,a_2\in\mathbb{Z}^n, \\ b_1,b_2\in\mathbb{R}^3, \\ ||b_1||_{I_3}=l}} \left(\left\| \begin{matrix} \hat{a}_1 - a_1 \\ \hat{a}_2 - a_2 \end{matrix} \right\|^2_{P\otimes Q_{\hat{a}}} + \left\| \begin{matrix} \hat{b}_1(a_1) - b_1 \\ \hat{b}_2(a_2) - b_2 \end{matrix} \right\|^2_{P\otimes Q_{\hat{b}(a)}} \right) \tag{21}$$

The last term on the right side can be rewritten as:

$$\left\| \begin{matrix} \hat{b}_1(a_1) - b_1 \\ \hat{b}_2(a_2) - b_2 \end{matrix} \right\|^2_{P\otimes Q_{\hat{b}(a)}} = \tag{22}$$

$$\left\| \hat{b}_1(a_1) - b_1 \right\|^2_{Q_{\hat{b}(a)}} + \left\| \hat{b}_2(a_2, b_1) - b_2 \right\|^2_{\frac{3}{4}Q_{\hat{b}(a)}}$$

With the constraint on the baseline b_1 and the ambiguities, the conditional solution of the baseline b_2 becomes:

$$\hat{b}_2(a_2, b_1) =$$

$$\hat{b}_2(a_2) - \left(-\frac{1}{2}Q_{\hat{b}(a)} \right) \left(Q_{\hat{b}(a)} \right)^{-1} \left(\hat{b}_1(a_1) - b_1 \right) \tag{23}$$

$$= \hat{b}_2(a_2) + \frac{1}{2} \left(\hat{b}_1(a_1) - b_1 \right)$$

The variance for this ambiguity constrained baseline is $D\left(\hat{b}_2(a_2, b_1) \right) = \frac{3}{4}Q_{\hat{b}(a)}$, and hence the knowledge of the constrained baseline allows us to improve the precision of the ambiguity constrained baseline from $Q_{\hat{b}(a)}$ to $\frac{3}{4}Q_{\hat{b}(a)}$. The integer least squares solution then becomes:

$$\begin{bmatrix} \check{a}_1 \\ \check{a}_2 \end{bmatrix} = \arg \min_{a_1,a_2\in\mathbb{Z}^n} \left(\left\| \begin{matrix} \hat{a}_1 - a_1 \\ \hat{a}_2 - a_2 \end{matrix} \right\|^2_{P\otimes Q_{\hat{a}}} + \right.$$

$$\left. + \min_{||b_1||=l} \left(\left\| \hat{b}_1(a_1) - b_1 \right\|^2_{Q_{\hat{b}(a)}} \right) \right)$$

$$\check{b}_1 = \arg \min_{||b_1||=l} \left(\left\| \hat{b}_1(\check{a}_1) - b_1 \right\|^2_{Q_{\hat{b}(a)}} \right)$$

$$\check{b}_2 = \hat{b}_2(\check{a}_2, \check{b}_1) = \hat{b}_2(\check{a}_2) + \frac{1}{2}\left(\hat{b}_1(\check{a}_1) - \check{b}_1 \right) \tag{24}$$

For which the ambiguity vector can also be written as:

$$\begin{bmatrix} \check{a}_1 \\ \check{a}_2 \end{bmatrix} = \arg \min_{a_1,a_2\in\mathbb{Z}^n} \left(\| \hat{a}_1 - a_1 \|^2_{Q_{\hat{a}}} + \right.$$

$$\left. \min_{||b_1||=l} \left(\| \hat{b}_1(a_1) - b_1 \|^2_{Q_{\hat{b}(a)}} \right) + \| \hat{a}_2(a_1) - a_2 \|^2_{\frac{3}{4}Q_{\hat{a}}} \right) \tag{25}$$

The first two terms of the right side of the equation form the ambiguity objective function for the constrained baseline as described in 4.2. The third term is due to the correlation between the ambiguities at the two baselines, where $\hat{a}_2(a_1) = \hat{a}_2 - \left(-\frac{1}{2}Q_{\hat{a}} \right)(Q_{\hat{a}})^{-1}(\hat{a}_1 - a_1) = \hat{a}_2 + \frac{1}{2}(\hat{a}_1 - a_1)$. This term contributes to the optimal solution but because of the low correlation we expect this contribution to be small.

The processing strategy makes use of the steps explained in section 4.1 and 4.2 of the standard and the baseline constrained LAMBDA method. We use the baseline constrained LAMBDA to enumerate the ambiguities of the constrained baseline b_1 in combination with ambiguity vectors for baseline b_2 using the correlation between the ambiguities on the two baselines. In the final step we will use eq. (24) to find the integer least squares solution.

5.4 SUBOPTIMAL SOLUTION OF THE FULLY INTEGRATED APPROACH (INTEGRATED APPROACH II)

An approximation of the integer least squares solution as given in the previous section can be obtained by treating the third term of eq. (25) as if it is uncoupled with the first two terms. That is, the above minimization would result in two uncoupled minimizations, one for a_1 and one for a_2, if the correlation would be absent. An approximation to the integer least-squares solution can in this way be obtained. The result is a vectorial bootstrapping approach in which we first solve the ambiguity on the constrained baseline and apply the found ambiguity vector in the solution of the unconstrained baseline. This is also the difference with the uncoupled approach from section 5.5 in which the solutions are found completely independent of each other. The overall solution is then given as:

$$\check{a}_1 = \arg \min_{a_1\in\mathbb{Z}^n} \left(\| \hat{a}_1 - a_1 \|^2_{Q_{\hat{a}}} + \right.$$

$$\left. + \min_{||b_1||=l} \left(\left\| \hat{b}_1(a_1) - b_1 \right\|^2_{Q_{\hat{b}(a)}} \right) \right)$$

$$\check{a}_2 = \arg \min_{a_2\in\mathbb{Z}^n} \left(\| \hat{a}_2(\check{a}_1) - a_2 \|^2_{\frac{3}{4}Q_{\hat{a}}} \right)$$

$$\check{b}_1 = \arg \min_{||b_1||=l} \left(\left\| \hat{b}_1(\check{a}_1) - b_1 \right\|^2_{Q_{\hat{b}(a)}} \right)$$

$$\check{b}_2 = \hat{b}_2(\check{a}_2) + \frac{1}{2}\left(\hat{b}_1(\check{a}_1) - \check{b}_1 \right) \tag{26}$$

For this approach in the first step we use the baseline constrained LAMBDA to estimate the ambiguities of the constrained baseline b_1. In the second step we use standard LAMBDA with $\hat{a}_2(\check{a}_1)$ and $\frac{3}{4}Q_{\hat{a}}$ on the unconstrained baseline. From eq. (26) and (25), it is expected that the success rate of the integer least squares (optimal) approach to be better than the vectorial bootstrapping (suboptimal) ap-

proach [14], but because of the low correlation between the two baselines the difference is anticipated to be minimal as discussed in the previous section. This is analyzed using simulated and field data in section 6.

It can be demonstrated that the suboptimal solution is the same as the solution from [15] in which the ambiguity vector for b_2 that minimizes the cost function in the metric of $Q_{\hat{a}}$ was found as:

$$\check{a}_2 = \arg \min_{a_2 \in \mathbb{Z}^n} \left(\|\hat{a}_2 - a_2\|^2_{Q_{\hat{a}}} + \right.$$
$$\left. + \|(\hat{a}_3 - a_1) - a_2\|^2_{Q_{\hat{a}}} \right) \tag{27}$$

5.5 UNCOUPLED APPROACH USING UNCONSTRAINED AND CONSTRAINED BASELINES

The simplest way to combine constrained and unconstrained baselines is the uncoupled approach in which the baselines are treated completely independently. This approach provides a lower bound for the empirical success rate of the optimal and suboptimal approaches described in the previous two sections.

6 EXPERIMENTAL VERIFICATION

In this section, the introduced methods are applied, using simulated and field data, to the most challenging application of single epoch, single frequency ambiguity resolution. We will investigate the experimental or empirical success rate, which depends on the strength of the underlying GNSS model. For analysis of the performance of the described methods, we compare the true integer ambiguity vector (the 'true solution' known in the simulations and estimated from post-processing for real data) and the estimated integer ambiguity vector at every epoch. The empirical success rate is defined as the number of epochs where the obtained integer ambiguity vector was equal to the true integer ambiguity vector divided by the total number of epochs. The baseline length, as long as the atmospheric affects on the GPS observations are negligible (typically if the baseline is shorter than 10 km, see [12]), will not influence the performance of the ambiguity resolution method. In this contribution we will simulate and analyze short baselines on a single platform, however the results will also apply to longer baselines (between different platforms) as long as the atmospheric influences are small. We will analyze both performance on individual baselines and on the solution of combined baselines (the "overall" solution). The first result is important as the information of the constrained baseline could improve the solution of the unconstrained baseline, and furthermore we would like to confirm that the success rate for the constrained baseline is not changed in the integrated solution compared to the standalone solution. The second result is important, as for

some applications, we are interested in the estimation of a number of baseline vectors on or between a number of platforms (see section 2.2).

6.1 SIMULATION SET UP

Date and time	22 Jan 2008 00:00
Location	Lat: 50° , Long: 3°
GPS week	439
Scenario	Dual baseline, orthogonal configuration stationary
Frequency	L1
Number of Satellites	5 - 6 - 7 - 8
Undifferenced code noise σ_p [cm]	30 - 15 - 5
Undifferenced phase noise σ_ϕ [mm]	3 - 1
Baseline length $\|b_1\| = \|b_2\| = l$	2.0 m
Epochs simulated	10^5

Table 1: Simulation specification

In order to investigate the performance of the proposed methods, we first analyze the empirical success rates using simulated data. Table 1 summarizes the conditions of the simulations. Utilizing the VISUAL software [16], based on the location of the receivers and an actual GPS constellation, the design matrices of the model are calculated. In order to obtain good approximations, the number of samples must be sufficiently large [17]. Assuming different levels of noise on the undifferenced phase (from 1 mm to 3 mm) and undifferenced code (from 5 cm to 30 cm) data, a set of 10^5 data was generated; then each simulation was repeated for different number of satellites varying between 5 and 8.

6.2 SIMULATION RESULTS

In this section we will analyze the three proposed integrated methods; uncoupled, suboptimal and optimal. The results are presented in three tables. Table 2, 3 and 4 contain empirical success rates as a function of the number of tracked satellites and the phase and code level noise (σ_ϕ, σ_p). In Table 2 and 3, we analyze the success rate on individual baselines, both standalone and as part of the (sub)optimal solution with $P(\check{a}_1 = a_1)$ for the constrained baseline b_1 and $P(\check{a}_2 = a_2)$ for the unconstrained baseline b_2.

In Table 2, we observe that the solution on the constrained baseline, as part of the optimal solution, has the same performance as the standalone baseline constrained solution. In the suboptimal solution, the constrained baseline is not influenced by the unconstrained baseline, hence the result
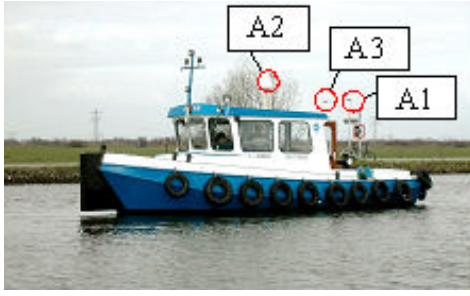
Fig. 3: Vessel Experiment, antenna definition

will be exactly the same as the standalone solution, and it is therefore not included in this table. In Table 3, the unconstrained baseline b_2 is presented as standalone and as part of the suboptimal and the optimal solution. As expected, when comparing Table 2 and 3, the baseline constrained solution clearly provides much better results than the unconstrained solution. The differences in success rate are particularly pronounced when the strength of the underlying GNSS model becomes weaker (fewer satellites and/or higher measurement noise). For the unconstrained baseline we observe that the (sub)optimal approach has a better performance than standalone. The improvement is between 0 and 13% with a larger improvement for weaker GNSS models. Furthermore we see that the optimal solution and the suboptimal solution have the same performance.

In Table 4, we look at the overall empirical success rate, which is the success rate on both baselines in a combined solution: $P(\check{a}_1 = a_1, \check{a}_2 = a_2)$. Again three methods using one constrained and one unconstrained baseline are considered: the uncoupled, the suboptimal and the optimal method. Compared to the uncoupled method, the improvement of the empirical success rate for the (sub)optimal solution is between 0 and 13%, with larger improvement for weaker GNSS models. Also for the overall success rate, the optimal solution and the suboptimal solution have the same performance.

6.3 EXPERIMENT SETUP

Next we will confirm the results of the simulated data using field data, which was collected onboard a vessel on the 3rd of April 2003 [18]. Fig. 3 shows the test setup of the experiment. For this experiment three dual frequency GPS receivers, two geodetic grade (Ashtech Z12 and Leica SR530 connected to antenna Ant_2 and Ant_1 in fig. 3 respectively) and one navigational type of receiver (NovAtel OEM3 connected to antenna Ant_3 in fig. 3) were utilized. The difference in accuracy of the observations is taken care of in the variance matrix. Data was collected at 1 Hz. Dual frequency observations are available for all receivers, but only single frequency observations (L1) will be analyzed. Fig. 5 shows the number of locked GPS satellites and PDOP for this data.

σ_ϕ [mm]	3			1		
σ_p [cm]	30	15	5	30	15	5
N	Standalone $P(\check{a}_1 = a_1)$					
	Optimal $P(\check{a}_1 = a_1)$					
5	0.72	0.89	1.00	0.97	1.00	1.00
	0.72	0.89	1.00	0.97	1.00	1.00
6	0.96	0.99	1.00	1.00	1.00	1.00
	0.96	0.99	1.00	1.00	1.00	1.00
7	0.99	1.00	1.00	1.00	1.00	1.00
	1.00	1.00	1.00	1.00	1.00	1.00
8	1.00	1.00	1.00	1.00	1.00	1.00
	1.00	1.00	1.00	1.00	1.00	1.00

Table 2: Simulation results: single-frequency, single-epoch success rates for the constrained baseline b_1

σ_ϕ [mm]	3			1		
σ_p [cm]	30	15	5	30	15	5
N	Standalone $P(\check{a}_2 = a_2)$					
	Suboptimal $P(\check{a}_2 = a_2)$					
	Optimal $P(\check{a}_2 = a_2)$					
5	0.03	0.19	0.87	0.06	0.27	0.95
	0.04	0.26	0.93	0.09	0.36	0.98
	0.04	0.26	0.93	0.09	0.36	0.98
6	0.25	0.67	0.97	0.49	0.87	1.00
	0.36	0.80	0.99	0.59	0.92	1.00
	0.36	0.80	0.99	0.59	0.92	1.00
7	0.50	0.80	1.00	0.75	0.93	1.00
	0.61	0.89	1.00	0.81	0.97	1.00
	0.61	0.89	1.00	0.81	0.97	1.00
8	0.86	0.95	1.00	1.00	1.00	1.00
	0.92	0.97	1.00	1.00	1.00	1.00
	0.92	0.97	1.00	1.00	1.00	1.00

Table 3: Simulation results: single-frequency, single-epoch success rates for unconstrained baseline b_2

σ_ϕ [mm]	3			1		
σ_p [cm]	30	15	5	30	15	5
N	Uncoupled $P(\check{a}_1 = a_1, \check{a}_2 = a_2)$					
	Suboptimal $P(\check{a}_1 = a_1, \check{a}_2 = a_2)$					
	Optimal $P(\check{a}_1 = a_1, \check{a}_2 = a_2)$					
5	0.02	0.17	0.86	0.05	0.27	0.95
	0.04	0.25	0.93	0.09	0.36	0.98
	0.04	0.25	0.93	0.09	0.36	0.98
6	0.24	0.66	0.97	0.49	0.87	1.00
	0.35	0.79	0.99	0.59	0.92	1.00
	0.36	0.79	0.99	0.59	0.92	1.00
7	0.50	0.80	1.00	0.75	0.93	1.00
	0.61	0.89	1.00	0.81	0.97	1.00
	0.61	0.89	1.00	0.81	0.97	1.00
8	0.86	0.95	1.00	1.00	1.00	1.00
	0.92	0.97	1.00	1.00	1.00	1.00
	0.92	0.97	1.00	1.00	1.00	1.00

Table 4: Simulation results: single-frequency, single-epoch overall success rates for two baselines
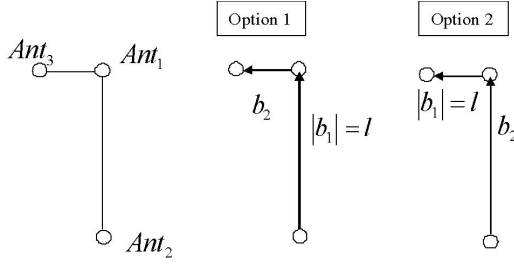
Fig. 4: Baseline definition

6.4 VESSEL RESULTS

The theoretical ambiguity success rate, i.e. probability of correct integer estimation, can be used to analyze the performance on the unconstrained baseline in the new integrated approach and therefore is introduced in this section based on [19]. As described in [14], a lower bound L_B of the probability of obtaining the correct integer ambiguity vector is:

$$P(\check{a} = a) \geq L_B(Bootstrapped) \qquad (28)$$

For an upper bound of the success rate we will make use of Ambiguity Dilution of Precision (ADOP). The ADOP is a diagnostic that tries to capture the main characteristics of the ambiguity precision. In Teunissen [20] it is proven that an upper bound U_B for the integer least squares success rate based on the ADOP can be given as:

$$P(\check{a} = a) \leq U_B(ADOP) \qquad (29)$$

Important to note is that these lower and upper bounds for ambiguity success rate are only valid for unconstrained baselines.

The lower and upper bound of the probability of obtaining the correct ambiguity vector can be used to analyze how much the success rate in theory could improve for the ambiguity estimator of the unconstrained baseline in the (sub)optimal solution compared to the standalone solution of the unconstrained baseline.

Fig. 6 and 7 show these lower and upper bounds of the success rate for $Q_{\hat{a}}$ and $\frac{3}{4}Q_{\hat{a}}$, where the former represents the baseline unconstrained solution, and the latter represents the unconstrained baseline in the (sub)optimal solution as described in eq. (24) and eq. (26). Only if the success rate of the constrained baseline is close enough to 1, then $\frac{3}{4}Q_{\hat{a}}$ is a good approximation of the variance matrix for the ambiguities on the unconstrained baseline. The difference between the lower and upper bound is on average about 9 % raised and this is the order of improvement we expect for the success rate.

Next we will analyze the empirical success rate of this data. The results are presented in three tables equivalent to the
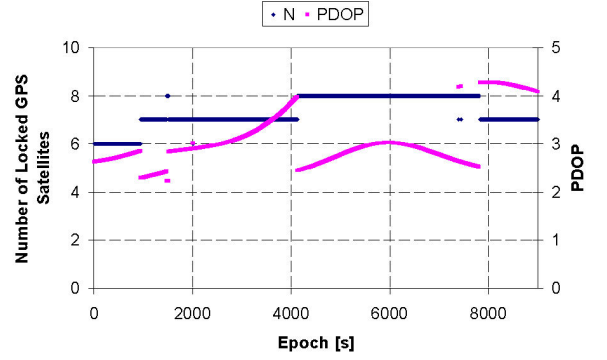
Fig. 5: Number of Locked satellites and PDOP
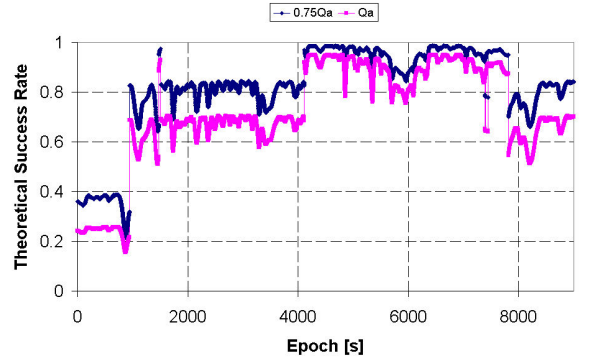
Fig. 6: Lower bound of the Success Rate for the unconstrained baseline in the standalone solution ($Q_{\hat{a}}$) and, in the (sub)optimal solution ($\frac{3}{4}Q_{\hat{a}}$)
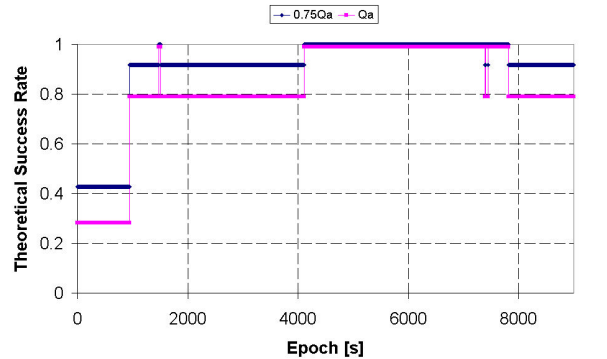
Fig. 7: Upper bound of the Success Rate for the unconstrained baseline in the standalone solution ($Q_{\hat{a}}$) and, in the (sub)optimal solution ($\frac{3}{4}Q_{\hat{a}}$)

ones used for the simulated results: Table 5 and 6 for individual baselines ($P(\check{a}_1 = a_1)$ and $P(\check{a}_2 = a_2)$) and Table 7 for overall success rate for two baselines ($P(\check{a}_1 = a_1, \check{a}_2 = a_2)$). We will analyze two options (defined in fig. 4) for which first one baseline is used as constrained and the other as unconstrained and in the second option we do

the opposite. Also here we observe that, for both option 1 and 2, the constrained baseline as a standalone solution and as part of the optimal solution have a similar performance. For option 2, the less accurate data from antenna Ant_3 is used on the constrained baseline. For option 1, it is used on the unconstrained baseline which explains the difference in performance of these baselines. Option 2 provides a better result for the unconstrained baseline and overall solution, as the less accurate data is used in the stronger (i.e. baseline constrained) model. The success rate on the unconstrained baseline is improved in the (sub)optimal solution compared to standalone, and the optimal and suboptimal solution have a similar performance. For option 1, the improvement is 8%, which is as expected from the raised lower and upper bounds for the success rates as shown in the beginning of this section. For option 2, the improvement is smaller as the success rate of the standalone solution was already much higher, since the stronger model (i.e. the baseline constrained model) applied to the data from the less accurate antenna. The overall success rate for two combined baselines is improved in the (sub)optimal solution compared to uncoupled solutions.

Success rate[%]	Option1	Option2
Standalone $P(\check{a}_1 = a_1)$	1.00	0.94
Optimal $P(\check{a}_1 = a_1)$	1.00	0.95

Table 5: Single-frequency, single epoch success rate for constrained baseline b_1

Success rate[%]	Option1	Option2
Standalone $P(\check{a}_2 = a_2)$	0.58	0.82
Suboptimal $P(\check{a}_2 = a_2)$	0.66	0.86
Optimal $P(\check{a}_2 = a_2)$	0.66	0.87

Table 6: Single-frequency, single epoch success rate for unconstrained baseline b_2

Success rate[%]	Option1	Option2
Uncoupled $P(\check{a}_1 = a_1, \check{a}_2 = a_2)$	0.58	0.78
Suboptimal $P(\check{a}_1 = a_1, \check{a}_2 = a_2)$	0.66	0.83
Optimal $P(\check{a}_1 = a_1, \check{a}_2 = a_2)$	0.66	0.83

Table 7: Single-frequency, single epoch overall success rate for two baselines

7 CONCLUSIONS

In this paper we explored methods for the combination of both relative positioning and attitude determination for moving platforms, each having multi-antennas with known baseline lengths. The objective of this research was to develop a rigorous method that optimally makes use of all the information available (the integerness of the ambiguities, the relationship between the ambiguities on the different baselines and the known baseline length of the constrained baselines) to determine the relative position and orientation of a multi-antenna system with unconstrained and constrained baselines. In order to obtain more insight into the problem we investigated an uncoupled and two integrated strategies (coined the integer least squares or optimal and vectorial bootstrapping or suboptimal approach) theoretically and experimentally. As was expected from the low correlation between the two baselines, the success rate of the integer least squares approach is similar to the vectorial bootstrapping approach. This was confirmed with simulated and field data for the single epoch, single frequency application. The developed methods are rigorous and have an additional advantage that they improve the ambiguity resolution on the unconstrained baseline and the overall success rate of ambiguity resolution between a number of antennas.

REFERENCES

[1] P J G Teunissen and A Kleusberg. GPS for Geodesy. *Springer, Berlin Heidelberg New York*, 1998.

[2] P J G Teunissen. The LAMBDA Method for the GNSS Compass. *Artificial Satellites, Vol.41,N.3*, 2006.

[3] P J G Teunissen. Integer Least Squares Theory for the GNSS Compass. *Journal of Geodesy, Springer, submitted*, 2008.

[4] P J G Teunissen. An Optimality Property of the Integer Least-Squares Estimator. *Journal of Geodesy*, 73(11):587–593, 1999.

[5] P J G Teunissen. Least Squares Estimation of the Integer GPS Ambiguities. *Invited lecture, Section IV Theory and Methodology, IAG General Meeting, Beijing*, 1993.

[6] P J G Teunissen. A New Method for Fast Carrier Phase Ambiguity Estimation. *Proceedings IEEE Position Location and Navigation Symposium, PLANS '94*, pages 562–573, 1994.

[7] C Park and P J G Teunissen. A New Carrier Phase Ambiguity Estimation for GNSS Attitude Determination Systems. *Proceedings of International GPS/GNSS Symposium, Tokyo*, 2003.

[8] P J Buist. The Baseline Constrained LAMBDA Method for Single Epoch, Single Frequency Attitude Determination Applications. *Proceedings of ION GPS-2007*, 2007.

[9] G Giorgi, P J G Teunissen, and P J Buist. A Search and Shrink Approach for the Baseline Constrained

LAMBDA: Experimental Results. *International Symposium on GPS/GNSS 2008, Tokyo, Japan, 11-14 November 2008, to be published*, 2008.

[10] G Blewitt. Carrier-phase ambiguity resolution for the Global Positioning System applied to baselines up to 2000 km. *Journal of Geophysical Research*, 94(B8):10187–10302, 1989.

[11] D Dong and Y Bock. Global Positioning System network analysis with phase ambiguity resolution applied to crustal deformation studies in California. *Journal of Geophysical Research*, 94(B4):3949–3966, 1989.

[12] P J Buist. GNSS Kinematic Relative Positioning for Spacecraft: Data Analysis of a Dynamic Testbed. *26th ISTS (International Symposium on Space Technology and Science, Hamamatsu, Japan, 1-8 June 2008*, 2008.

[13] P J G Teunissen. A General Multivariate Formulation of the Multi-Antenna GNSS Attitude Determination Problem. *Artificial Satellites, Vol.42,N.2*, 2007.

[14] P J G Teunissen. Success probability of integer GPS ambiguity rounding and bootstrapping. *Journal of Geodesy*, 72:606–612, 1998.

[15] J Pinchin, C Hide, D Park, and X Q Chen. Precise Kinematic Positioning Using Single Frequency GPS Receivers and an Integer Ambiguity Constraint. *Proceedings of IEEE PLANS 2008*, 2008.

[16] S Verhagen. Visualization of GNSS-related design parameters: Manual for the Matlab user interface VISUAL. 2006.

[17] P J G Teunissen. On the integer normal distribution of the GPS ambiguities. *Artificial Satellites*, 33(2):49–64, 1998.

[18] M O Kechine, C C J M Tiberius, and H van der Marel. *Experimental Verification of Internet-based Global Differential GPS*. Proceedings of ION-GPS/GNSS-2003, 2003.

[19] S Verhagen. On the approximation of the integer least-squares success rate: which lower or upper bound to use? *Journal of Global Positioning Systems*, 2(2):117–124, 2003.

[20] P J G Teunissen. ADOP based upperbounds for the bootstrapped and the least-squares ambiguity success rates. *Artificial Satellites*, 35(4):171–179, 2000.